Published in final edited form as:
NMR Biomed. 2012 February ; 25(2): 271–278. doi:10.1002/nbm.1745.

In Vivo Magnetic Resonance Studies of Glycine and Glutathione Metabolism in a Rat Mammary Tumor

Peter E. Thelwall[a], **Nicholas E. Simpson**[b], **Zahid N. Rabbani**[c], **M. Daniel Clark**[d], **Roxana Pourdeyhimi**[e], **Jeffrey M. Macdonald**[e], **Stephen J. Blackband**[d], and **Michael P. Gamcsik**[e,*]

[a]Newcastle Magnetic Resonance Centre, Campus for Ageing and Vitality, Newcastle University, Newcastle upon Tyne, UK

[b]Department of Medicine, Division of Endocrinology, University of Florida, Gainesville, FL, USA

[c]Department of Radiation Oncology, Duke University Medical Center, Durham, NC

[d]Department of Neuroscience, University of Florida, Gainesville, FL, USA

[e]Joint Department of Biomedical Engineering, University of North Carolina, Chapel Hill and North Carolina State University, Raleigh, NC, USA

Abstract

The metabolism of glycine into glutathione was monitored noninvasively *in vivo* in intact R3230Ac rat tumors by magnetic resonance imaging and spectroscopy. Metabolism was tracked by following the isotope label from intravenously infused [2-^{13}C]-glycine into the glycinyl residue of glutathione. Signals from [2-^{13}C]-glycine and γ-glutamylcysteinyl-[2-^{13}C]-glycine (^{13}C-glutathione) were detected by nonlocalized ^{13}C spectroscopy as these resonances are distinct from background signals. In addition, using spectroscopic imaging methods, heterogeneity in the *in vivo* tumor distribution of glutathione was observed. *In vivo* spectroscopy also detected isotope incorporation from [2-^{13}C]-glycine into both the 2- and 3-carbons of serine. Analyses of tumor tissue extracts show single and multiple label incorporation from [2-^{13}C]-glycine into serine from metabolism through the serine hydroxymethyltransferase and glycine cleavage system pathways. Mass spectrometric analysis of extracts also shows that isotope-labeled serine is further metabolized *via* the transsulfuration pathway as the ^{13}C-isotope labels appear in both the glycinyl- and the cysteinyl-residue of glutathione. Our studies demonstrate the use of magnetic resonance imaging and spectroscopy for monitoring tumor metabolic processes central to oxidative stress defense.

Keywords

glutathione; magnetic resonance; serine; metabolism; transsulfuration

INTRODUCTION

Proliferating tissues in general, and tumor cells in particular, exhibit highly reduced intracellular environments that are characterized by high levels of reduced glutathione compared to its oxidized disulfide counterparts (1). In many clinical studies, higher levels of glutathione and its associated enzymes appear to play a significant role in therapy-resistance (2) and reduced overall survival (3). However, a number of clinical studies have failed to

*Correspondence to; M. Gamcsik, PhD; 4206D Engineering Bldg 3; Campus Box 7115, NC State University, Raleigh, NC 27695-7115; Phone: (919) 513-0786; FAX: (919) 513-7601; mgamcsi@ncsu.edu.

demonstrate a clear relationship between glutathione levels and clinical outcome (e.g. (4)). These mixed results may reflect the difficulty in obtaining biopsy specimens truly reflective of total tumor biochemistry. For example Barranco et al., (5) found an accurate representation of tissue glutathione requires 3–7 biopsy samples per tumor. This level of tissue sampling is often impractical in the clinical setting and noninvasive measures of glutathione heterogeneity would be preferable. In addition, studies on drug-sensitive and resistant cancer cells in our laboratory showed that the rate of glutathione metabolism may be a significant factor in therapy response (6,7). The high levels of glutathione found in some tissues enable noninvasive monitoring of glutathione metabolism in intact cultured cells (6,8) and *in vivo* in liver (9) and in tumor xenografts (10). In the latter study, we used ^{13}C magnetic resonance spectroscopic imaging to detect the distribution of glutathione in subcutaneously implanted fibrosarcomas in rats that were infused with ^{13}C-glycine (10). This fibrosarcoma exhibited high levels of glutathione (>2 mmol/gram-tissue), facilitating detection. In order to extend these studies to different tumor types with lower glutathione levels, we now report on the noninvasive detection of glutathione in a rat mammary R3230Ac adenocarcinoma. These tumors have lower average levels of glutathione as compared to the fibrosarcomas, a distinct disadvantage to obtaining useful magnetic resonance data. Nonetheless, metabolite levels and label incorporation are high enough to allow *in vivo* magnetic resonance detection of glutathione metabolism. Furthermore, *in vivo* spectroscopy detected [2-^{13}C]-glycine metabolism into serine *via* the action of serine hydroxymethyltransferase and the glycine cleavage system; an important pathway providing building blocks for one-carbon metabolism. Examination of tissue extracts by mass spectrometry and high-resolution magnetic resonance spectroscopy found that further metabolism of serine into cysteine occurs through the transsulfuration pathway resulting in multiple isotope labeling of part of the glutathione pool in both the glycinyl- and cysteinyl-moieties. These studies demonstrate that isotope-labeled glycine offers a probe of multiple processes key to maintenance of oxidative stress defenses in tumor tissue.

MATERIALS AND METHODS

[2-^{13}C]-Glycine was purchased from Cambridge Isotope Laboratories, Inc. (Andover, MA). Monobromobimane was obtained from Calbiochem (San Diego, CA). N-Ethylmaleimide was from Sigma Chemical Co. (St. Louis, MO).

The Animal Care and Use Committees of the University of Florida and the University of North Carolina approved the procedures used in these studies. Rat mammary tumor tissue R3230Ac was provided by Dr. Mark Dewhirst of Duke University. Fresh R3230Ac tissue fragments from donor rats were implanted into the flank of female Fischer 344 rats and grew into 0.5 to 1.0 cm^3 tumors within 3 weeks. For glycine infusion, a catheter was implanted into the external jugular vein of the rats and exteriorized between the scapulae. A fitted harness (Instech-Salomon, Plymouth Meeting, PA) and infusion lines allowed free movement throughout the cage during the infusion. Sterile solutions of [2-^{13}C]-glycine were prepared in saline, adjusted to pH 7.4 and infused at a rate of 0.5 or 1.0 mmol/kg/h (0.5 mL/h) using a syringe pump.

Magnetic resonance data were acquired using an 11.0 T, 40-cm bore diameter horizontal superconducting magnet (Magnex Scientific, Oxfordshire, UK) interfaced to a Bruker (Billerica, MA) spectrometer and console. A 1.2 cm diameter three turn surface coil tuned to the ^{13}C frequency (118 MHz) was placed against or around the tumor. An orthogonally-oriented 3 cm diameter single turn surface coil was positioned below the tumor and tuned to the ^{1}H frequency (470 MHz) for ^{1}H imaging and decoupling. Rats were initially anesthetized with 5% isoflurane/oxygen and maintained with 2% isoflurane/oxygen. Animals were placed on a heating pad in a magnetic resonance-compatible cradle during

imaging to maintain body temperature. Tumor tissue was harvested at the conclusion of all magnetic resonance experiments, immediately frozen in liquid nitrogen, and stored at −80 °C.

Non-localized ^{1}H-decoupled ^{13}C spectra were acquired using a pulse-acquire sequence with ^{1}H WALTZ-decoupling during the acquisition period. A nominal 90° tip from a rectangular RF excitation pulse was employed. Data were acquired into 1024 datapoints over a spectral width of 10 kHz and a relaxation delay of 1.5 sec, 400 averages, yielding a scan duration of 10 min.

2D ^{13}C chemical shift imaging (CSI) scans were acquired into an 8 × 8 phase encode matrix over a field of view of 2.4 × 2.4 cm. A variable k-space averaging pulse sequence was used with 1:128 averages per phase encoding step. Excitation, acquisition and decoupling parameters were the same as for acquisition of non-localized spectra. The repetition time was 1.5 sec and the total scan duration was 72 minutes. Data were reconstructed into a 16 × 16 matrix and 40 Hz exponential line broadening applied. Data processing was performed using in-house software developed in Matlab (The MathWorks, Inc. Natick, MA, USA).

The *in vitro* high-resolution magnetic resonance data were collected on a Bruker Avance 11.75 T spectrometer with direct detection of ^{13}C with ^{1}H decoupling with pulse widths and repetition times similar to those used *in vivo*. Correlations between ^{13}C and ^{1}H resonances were obtained from ^{1}H-detected heteronuclear single quantum coherence (HSQC) experiments performed on a Varian Inova 16.5 T spectrometer (11).

All high-resolution magnetic resonance data were obtained from monobromobimane-treated tissue samples extracted with perchloric acid as described below.

Reduced glutathione and cysteine were measured as their bimane adducts by liquid chromatography. Frozen tumor tissue sections were homogenized in preweighed solutions of 0.05 M phosphate buffer containing 50 mM acivicin and 5 mM monobromobimane at room temperature. Proteins were precipitated by the addition of perchloric acid and removed by centrifugation. The thiol-bimane conjugates in the KOH-neutralized acid extracts were analyzed on a Waters Acquity Ultra Performance Liquid Chromatography system with spectrophotometric detection at 390 nm. Metabolite levels are expressed relative to the mass of the frozen tissue extracted. At least three samples of between 5–50 mg each were obtained from each tumor and extracted. Extraction of tissue for high-resolution magnetic resonance studies (e.g. Fig. 4) was performed as outlined above using tissue samples of 200–300 mg.

Oxidized glutathione disulfide (GSSG) content was determined by two methods. The monobromobimane-treated extract was adjusted to pH 8.8 and treated with dansylchloride. Reverse-phase liquid chromatography was used to detect bis-dansyl-GSSG in the extract at 333 nm. In addition, GSSG was detected and quantitated by mass spectrometry in samples treated with N-ethylmaleimide (see below).

Isotopic enrichment data and assay of reduced and oxidized glutathione were obtained by trapping reduced glutathione using N-ethylmaleimide. Briefly, frozen tissue tumor fragments were suspended in 10 mM N-ethylmaleimide in distilled water and tissue dispersed with a Polytron tissue homogenizer. After sitting at room temperature for 15 minutes, suspended solids were removed by centrifugation and the supernatant analyzed by liquid chromatography/mass spectrometry in the Genome Sciences Laboratory of NC State University. Mass spectrometric analyses were performed with a Thermo Surveyor liquid chromatograph coupled to a Thermo LTQ linear ion trap mass spectrometer. Chromatographic separations were achieved with a Thermo Hypersil Gold: 150mm ×

2.1mm I.D., 5um particle size, 175Å pore size reverse-phase column. The mobile phase composition was programmed with a solvent gradient, initial conditions of 250 mL/min with a mixture of 97% acidified water (50 mM acetic acid) and 5% acetonitrile programmed to hold at initial conditions for 3.5 minutes, followed by a linear ramp to a final mixture of 15% acidified water and 85% acetonitrile over the course of 9.5 minutes. The mass spectrometer was operated in positive ion mode with electrospray ionization. The integrated intensities of the peaks at mass-to-charge (*m/z*) 433 (M+H), *m/z* 434 and *m/z* 435 due to *S*-(N-ethylmaleimidyl)-glutathione were measured and converted to fractional abundance. Similarly, the isotopic distribution in cysteine in the tissue samples was calculated by analyzing the isotope distribution pattern for the *S*-(N-ethylmaleimidyl)-cysteine at *m/z* 247, 248, 249. The amount of oxidized glutathione disulfide was determined by comparing the intensity of the *m/z* 613 to known concentration standards. Identification of amino acid enrichment sites in glutathione was determined by collecting tandem mass spectrometry data for the peak at *m/z* 435.

The theoretical isotope distribution pattern for *S*-(N-ethylmaleimidyl)-glutathione ($C_{16}N_4O_8H_{24}S$) was calculated using a mass spectrometry webtool (12). Using this webtool, the natural abundance isotope distribution pattern is 1.0, 0.202, 0.0797 for *m/z* 433, 434, 435, respectively. For 100% enriched with a single ^{13}C-label ($^{13}C_1$-glutathione), the pattern generated is 1.0, 0.192, 0.0776 for *m/z* 434, 435, 436, respectively. For 100% enriched with two ^{13}C-labels, i.e. $^{13}C_2$-glutathione, the patterns are 1.0, 0.181, 0.0757 for *m/z* 435, 436, 437. Theoretical enrichment patterns were generated *in silico* from linear combinations of mixtures containing natural abundance glutathione and $^{13}C_1$-glutathione that had been enriched with between 0.5 and 50% single ^{13}C. In addition, theoretical enrichment patterns were generated for tertiary mixtures of natural abundance, 0.5 – 50% $^{13}C_1$-glutathione, 0.5 – 10% $^{13}C_2$-glutathione. These theoretical data were fit to the isotope enrichment measurements of *S*-N-ethylmaleimidyl-glutathione and *S*-N-ethylmalimidyl-cysteine in tumor tissue samples, by an approach analogous to our previously described methods for *S*-bimane-glutathione (7).

Frozen tumor tissue was sectioned in the same orientation as the MR imaging plane. Two adjacent sections were stained separately with Mercury Orange (13) and Hematoxylin-Eosin. Images were captured, digitized and analyzed with MetaMorph (Universal Imaging Corp., Downingtown, PA), Matlab (The Mathworks, Inc., Natick, MA) and Adobe Photoshop (Adobe Systems, Inc., San Jose, CA) software.

RESULTS

Metabolite Levels

The glutathione or cysteine levels in extracts prepared from R3230Ac tumor tissues from rats infused with 0.5 or 1.0 mmol/kg/h mmol/kg/h [2-^{13}C]-glycine were not significantly different from levels in R3230Ac tumor tissues from control rats not infused with glycine (Table 1). Levels of oxidized glutathione disulfide were 0.00528 ± 0.00252 mmol/g-tissue (n = 4) for rats infused with 0.5 mmol/kg/h [2-^{13}C]-glycine, approximately 0.4% of the reduced glutathione level.

Unlike the glutathione and cysteine levels, infusion of [2-^{13}C]-glycine altered the glycine and serine concentrations in the tumor tissue (Table 1). The glycine levels increase 1.6-fold when infused at 0.5 mmol/kg/h and further increase by 2.1-fold at the 1.0 mmol/kg/h [2-^{13}C]-glycine infusate level. Serine shows a similar increase from controls when 0.5 mmol/kg/h [2-^{13}C]-glycine was infused but did not change substantially when the infusate concentration was raised to 1.0 mmol/kg/h.

In Vivo Magnetic Resonance Spectroscopy

Figure 1 shows *in vivo* non-localized ^{13}C spectra from a subcutaneously implanted R3230Ac tumor before (Fig. 1A) and after 30 hours of [2-^{13}C]-glycine infusion at a rate of 0.5 mmol/kg/h (Fig. 1B). Several broad envelopes of resonances centered at approximately 15, 30 and 63 ppm are primarily due to subcutaneous and tumor lipids and are visible in both spectra. After 30 hours of [2-^{13}C]-glycine infusion (Fig. 1B), a new set of resonances is visible between 42 and 45 ppm. The resonance of the infused [2-^{13}C]-glycine appears at 42.4 ppm (Gly, Fig. 1), and incorporation of this labeled amino acid into the glycinyl-residue of glutathione shifts the position of the ^{13}C resonance to 44.2 ppm. For brevity, we will refer to glutathione with [2-^{13}C]-glycine incorporated into the glycinyl-residue as (2-^{13}C-gly)-GSH (Fig. 1). A broader resonance between these two is thought to be [2-^{13}C]-glycine incorporated into other cellular large peptides and proteins (see below). As a comparison, spectra in Figure 1C show data from an analogous study that employed 24 h of [2-^{13}C]-glycine infusion at the higher concentration of 1.0 mmol/kg/h. The higher intensity of both the [2-^{13}C]-glycine and (2-^{13}C-gly)-GSH is evident.

In addition to the peaks assignable to [2-^{13}C]-glycine and (2-^{13}C-gly)-GSH, additional resonances are detectable at 54.8, 57.4 and 61.3 ppm, with the resonance at 61.3 ppm overlapping the background signal. Extract data analysis (below) enabled assignment of these resonances to [2-^{13}C]-creatine (54.8 ppm), [2-^{13}C]-serine (57.4 ppm) and [3-^{13}C]-serine (61.3 ppm).

The spectra shown in Fig. 1 are representative of the metabolite distribution across the tumor and do not provide a measure of tissue distribution. Chemical shift imaging (CSI), performed in one-, two- or three-dimensions can provide spectral information with spatial location. Attempts to perform localized spectroscopy by 1D and 2D CSI did not yield data with sufficient signal for quantification in a reasonable scan duration (<90 min) from tumors in rats infused with 0.5 mmol/kg/h [2-^{13}C]-glycine for periods of between 24 and 46 hours. Increasing the infusate concentration to 1.0 mmol/kg/h [2-^{13}C]-glycine enabled localized spectroscopy in these tumors. An example of localized magnetic resonance data is shown in Figure 2. Figure 2A shows the ^{1}H image of an R3230Ac tumor with a 16 × 16 localization matrix over which the CSI data is collected. The 2D CSI data obtained from each region of the matrix is shown in Figure 2B. For clarity, only the portion of the ^{13}C spectrum showing the glutathione and glycine resonances (between 40.8 and 45.5 ppm) are shown. From these data, both the [2-^{13}C]-glycine image (Fig. 2C) and (2-^{13}C-gly)-GSH image (Fig. 2D) were generated. The ^{13}C signal available in these tumors was insufficient for collection of a 3D data set. Because of this, the signal intensities in both Figures 2C and 2D are brighter in the center of the tumor due to the greater tissue thickness compared to the tumor periphery. The ratio of glutathione to glycine at each pixel was determined as an indicator of glutathione synthesis rate that is independent of tissue thickness. Integrated peak areas for glycine and glutathione were calculated and an image generated from these data (Fig. 2E). This ratio image shows the variation in the amount of (2-^{13}C-gly)-GSH synthesized across the tumor normalized to the delivered [2-^{13}C]-glycine.

Tumor Histology

After localized *in vivo* magnetic resonance studies, the imaging plane was marked on each tumor and the tissue was frozen for histological analysis. Thin tumor sections were obtained from the central part of the R3230Ac tumors and treated with Hematoxylin-Eosin (Fig. 3A). An adjacent tissue section was treated with the fluorescent glutathione reagent Mercury Orange under conditions that minimize nonspecific staining from other cellular thiols (13). Thin sections from R3230Ac tumors stained with Mercury Orange consistently show

heterogeneity in fluorescence intensity due to variation in glutathione concentration across the tumor. A representative example is shown in Fig. 3B.

Mass Spectrometry

Isotope Fractional Enrichment: The glutathione extracted from tumor tissue was analyzed by mass spectrometry. Experimental data was compared to theoretical mass spectral data generated from mixtures containing only natural abundance (unenriched) glutathione, 100% enriched at one carbon atom with ^{13}C, i.e. $^{13}C_1$-glutathione and linear combinations of both. For example, natural abundance unenriched glutathione isolated from a control R3230Ac tumor showed an isotope distribution of 1.00, 0.200 and 0.0825 for the *m/z* peaks at 433, 434 and 435, respectively. This closely matches the theoretical isotope distribution of 1.00, 0.202 and 0.0797 for *S*-N-ethylmaleimidyl-glutathione (12). In all tumors studied, the fit between the experimental data and theoretical data for glutathione enriched with a single carbon was unsatisfactory. Only by including a tertiary mixture of natural abundance, $^{13}C_1$-glutathione and doubly labeled glutathione ($^{13}C_2$-glutathione), did the experimental isotope distribution patterns match well with the theoretical patterns. For five R3230Ac tumors infused for an average of 40.2 ± 5.9 hours with 0.5 mmol/kg/h [2-^{13}C]-glycine, the fraction of $^{13}C_1$-glutathione was 0.293 ± 0.015 and the fraction of $^{13}C_2$-glutathione was 0.0023 ± 0.008 above natural abundance levels. For three tumors infused for an average of 25.5 ± 1.3 hours, the fraction of $^{13}C_1$-glutathione was 0.232 ± 0.014 and the fraction of $^{13}C_2$-glutathione was 0.0015 ± 0.0005. For three tumors infused for an average of 22.4 ± 3.2 hours with 1.0 mmol/kg/h [2-^{13}C]-glycine, the fraction of $^{13}C_1$-glutathione was 0.387 ± 0.015 and the fraction of $^{13}C_2$-glutathione was 0.0026 ± 0.0006.

Since the magnetic resonance data shows most of the ^{13}C-label in glutathione is in the glycinyl-residue, tandem mass spectrometry was performed to identify the amino acid location of the second carbon label. These data (not shown) indicated the glycinyl- and cysteinyl-residues are the sites of enrichment in $^{13}C_2$-glutathione.

These data indicate a proportion of the cysteine had become ^{13}C-enriched prior to incorporation into glutathione. Mass spectrometry was used to calculate enrichment of the cysteine pool in the tumor tissue. For three tumors infused for 22.4 h with 1.0 mmol/kg/h [2-^{13}C]-glycine the fractional enrichment of $^{13}C_1$-cysteine was 0.0267 ± 1.15.

In Vitro Magnetic Resonance Spectroscopy

Tumors were frozen and monobromobimane-treated perchloric acid extracts were prepared at the conclusion of the *in vivo* spectroscopy experiments. Treatment with monobromobimane blocks oxidation of glutathione and does not significantly affect the chemical shift of most of the observed resonances. The high-resolution magnetic resonance spectrum acquired from a perchloric acid extract of a tumor is shown in Figures 4A and B. The [2-^{13}C]-glycine resonance at 42.4 ppm and the resonance from bimane-conjugated glutathione enriched in the 2-carbon of the glycinyl residue ((2-^{13}C-gly)-GSH-bim) at 44.2 ppm, dominate the spectrum. A notable difference between the *in vivo* spectrum in Figure 1C and the extract spectra in Figure 4A is the absence of a peak located between the [2-^{13}C]-glycine and (2-^{13}C-gly)-GSH-bim resonances. We postulate that this *in vivo* resonance arises from the incorporation of [2-^{13}C]-glycine into some of the tissue proteins. Preparation of perchloric acid extracts would remove these proteins, eliminating their resonances from the *in vitro* spectra.

Enrichment in two of the carbons of serine is visible as resonances at 57.4 ppm due to [2-^{13}C]-serine, and at 61.3 ppm from [3-^{13}C]-serine. Both of these peaks show additional complexity due to one-bond ^{13}C-^{13}C scalar coupling, indicating the presence of some

[2,3-$^{13}C_2$]-serine (Figure 4B). A singly labeled serine molecule leads to the central peak in these multiplets and doubly labeled [2,3-$^{13}C_2$]-serine appears as 'satellites' on either side of the central peak resulting in a triplet appearance for both peaks. An additional significant resonance shown in the extract spectrum is at 54.8 ppm. Possible metabolites for the peak at 54.8 ppm could be either [$^{13}CH_3$]-choline or [2-^{13}C]-creatine. Using a ^{1}H-(^{13}C)-HSQC experiment, the 54.8 ppm ^{13}C peak is correlated to a ^{1}H peak at 3.93 ppm indicating that in these tumors, the label from [2-^{13}C]-glycine is metabolized to [2-^{13}C]-creatine (data not shown) (14).

The mass spectroscopy results suggest that some of the label from [2-^{13}C]-glycine ends up in labeling the cysteinyl-residue of glutathione. Close inspection of the tumor extract data shows a small resonance due to incorporation as glutathione labeled in the 2-position of the cysteinyl-residue ((2-^{13}C-cys)-GSH-bim) and somewhat less label in the 3-position ((3-^{13}C-cys)-GSH-bim) just detectable in the spectrum (Fig. 4A). The assignment of these resonances is detailed below.

The incorporation of a ^{13}C label from [2-^{13}C]-glycine into cysteine occurs *via* the transsulfuration pathway with labeled serine as an intermediate. Since transsulfuration is a significant pathway in liver (15), we expect liver tissue from [2-^{13}C]-glycine-infused rats to also show significant cysteine labeling. The extracts of liver tissue from the [2-^{13}C]-glycine-infused tumor-bearing rats were examined by magnetic resonance spectroscopy. The ^{13}C spectrum of such a liver sample is shown in Figures 4C and D. In this spectrum, the more rapid synthesis of glutathione in liver is evident as a pronounced incorporation of label from [2-^{13}C]-glycine into the glutathione ([2-^{13}C-gly]-GSH-bim) peak at 44.2 ppm. A number of additional peaks are evident in this spectrum and not all peaks have been assigned. As observed in ^{13}C spectra of tumor tissue extracts, significant labeling is detected at 57.4 ppm from [2-^{13}C]-serine and at 61.3 from [3-^{13}C]-serine. The liver sample also shows the presence of multiply labeled serine as evident by the complex signals due to the ^{13}C-^{13}C scalar coupling (Figure 4D).

Transsulfuration in the liver should lead to cysteine, and subsequently glutathione, labeled primarily as [2-^{13}C]-cysteinyl-glutathione-bimane ([2-^{13}C-cys]-GSH-bim) and smaller amounts in [3-^{13}C]-cysteinyl-glutathione-bimane ([3-^{13}C-gly]-GSH-bim). In Figure 4C a resonance at 53.8 ppm and a smaller resonance at 34.3 ppm are likely candidates for the bimane-conjugated [2-^{13}C]-cysteinyl- and [3-^{13}C]-cysteinyl-glutathione-bimane, respectively. These conjugates are formed when monobromobimane is added to tissue extracts to prevent oxidation of reduced glutathione. In contrast to the minimal effect of the bimane reaction on the chemical shifts of the glycinyl-resonances, the site of bimane reaction occurs on the nearby thiol group resulting in a greater change in the chemical shifts of cysteinyl-resonances. From a two-dimensional ^{1}H-(^{13}C)-HSQC experiment, the peak at 53.8 ppm in the ^{13}C-spectrum correlates to a distinct proton resonance at 4.58 ppm, corresponding to the α-proton of the cysteinyl-residue of the glutathione-bimane conjugate (data not shown). The peak at 34.3 ppm in the ^{13}C-spectrum correlates to two sets of proton resonances at 3.23 and 2.97 ppm that are characteristic for the β-proton resonances for the cysteinyl-residue of the glutathione-bimane conjugate (16). These peaks are not due to natural abundance glutathione as spectra obtained under identical conditions on extracts taken from similar amounts of liver tissue from control rats do not show these peaks. These HSQC data confirm that ^{13}C label appears in both the 2- and 3-positions of the cysteinyl residue of glutathione at 53.8 and 34.3 ppm, respectively. Close inspection of these cysteinyl-glutathione-bimane peaks at 53.8 and 34.3 ppm show similar ^{13}C-^{13}C scalar coupling patterns in these cysteinyl residues as those found in serine. The grey lines Figure 4C point out the similarity in the appearance the [2-^{13}C]- and [3-^{13}C]-serine peaks linked to the downstream metabolites for those same carbons in the cysteinyl-residue of glutathione.

Not only is labeled cysteine taken up into glutathione but a portion of this amino acid is shunted into isotope labeled to taurine (Fig. 4C). These assignments were confirmed from ^{1}H-(^{13}C)-HSQC and are above natural abundance levels (data not shown). Cysteine itself is not detectable under these experimental conditions due to its low concentration in the tissues.

DISCUSSION

The mean glutathione concentration in the R3230Ac tumors was 1.22 mmol/g-tissue, 59% of the level found in our earlier study of the FSA fibrosarcoma xenografts. Glutathione levels in both the R3230Ac tumors and the FSA fibrosarcoma xenografts were unaffected by glycine infusion at the concentrations employed demonstrating that the ^{13}C label can be introduced by [2-^{13}C]-glycine infusion without significantly altering glutathione metabolism. Our earlier studies showed glycine infusion did not affect rat well-being, and did not perturb blood counts or serum electrolyte levels (10).

Detection of glutathione by *in vivo* ^{13}C magnetic resonance methods requires incorporation of a significant fraction of ^{13}C-label into the tripeptide. The amount of label incorporated is a function of the rate at which glutathione is metabolized and the fractional enrichment of the metabolic substrates. The fraction of the glutathione pool containing ^{13}C label after infusion at 0.5 mmol/kg/h for 40 h (0.293 ± 0.015) is similar to that observed earlier in the FSA tumors (0.292 ± 0.024) (10). Since the FSA tumors had higher glutathione steady state glutathione content, the amount of glutathione synthesized in the FSA tumor was almost twice that of the R3230Ac xenografts. The similar fractional enrichment between the two different tumors likely means an isotopic steady-state has been reached where the glutathione enrichment reflects the enrichment of the glycine pool which should be similar for rats infused with the same level of [2-^{13}C]-glycine. In the R3230Ac tumor studies reported here, the lower concentrations of ^{13}C-labelled glutathione, and thus lower signal in spectra, were manifest as lower signal-to-noise ratio (SNR). In previous studies of the FSA tumor, both 1D and 2D localized spectroscopy could be performed after 12 h of infusion [2-^{13}C]-glycine at a rate of 0.5 mmol/kg/h. This was not practically achievable in the R3230Ac tumors. Although nonlocalized data could be acquired at this infusion rate, acceptable SNR in 1D and 2D CSI experiments on the R3230Ac tumors could only be obtained after infusion of [2-^{13}C]-glycine at a rate of 1.0 mmol/kg/h.

Acquisition of a complete 2D-CSI data set shown in Figure 2, with the in-plane resolution of 1.5 mm, required a scan of 72 minutes duration. The SNR from ^{13}C-glutathione was not sufficiently high to attempt a 3D-CSI data set. By taking a ratio of the resonance intensities for glutathione and glycine (Fig. 2E), we can account for differences in tissue thickness since ^{13}C-glutathione can only be produced from regions of the tumor receiving [2-^{13}C]-glycine. The thicker the tissue sampled, the more [2-^{13}C]-glycine is likely to be detected and for regions where glycine cannot penetrate, glutathione would also be undetectable. The ratio map reflects regions where RF coil sensitivity and ^{13}C-glutathione concentration combine to provide sufficient SNR for detection. Similar to our results with the FSA tumor (10), heterogeneity in ^{13}C-labeled glutathione content is apparent. Previous studies of R3230Ac tumors have demonstrated heterogeneity in glucose consumption and oxygenation (17), and our histology data showing heterogeneity of glutathione concentration show a similar pattern of metabolic heterogeneity (Figure 3).

The lower glutathione concentration observed in R3230Ac compared to our previous studies of FSA tumors compounds the difficulty of attaining *in vivo* ^{13}C-glutathione images. Thus our data are necessarily acquired without slice selection, making direct comparison with histological data difficult. Although direct comparison between histology and *in vivo* images

are hampered by the inability to acquire slice selective 2D CSI data, Figure 2E supports our conclusion that the relative amounts of glutathione and glycine are heterogeneous, as uniform distrubutions of glycine and glutathione content would result in a homogeneous ratio map. A full 3D CSI dataset would allow us to fully characterize metabolic heterogeneity across the tumor, providing information equivalent to our histology data. We are developing RF coil and scan protocol improvements to increase ^{13}C SNR, and thus allow acquisition of slice-selective 2D ^{13}C datasets better suited to quantifying glutathione content and spatial heterogeneity. Studies have demonstrated elevated glutathione content occurs in hypoxic regions of cervical carcinoma xenografts (18), though other reports of human tumor tissues (19) and cancer cell lines (20) have found no consistent relationship between oxygen levels and glutathione content. Thus the further development of our *in vivo* ^{13}C imaging methods (combined with correlative measures of tissue metabolism) have the potential to provide information on how tumor microenvironment alters tissue oxidative stress defences.

The *in vivo* magnetic resonance data does not have the capability to distinguish between reduced and oxidized glutathione disulfide as the C2-carbon resonance of the glycyl-residue for these two species differ by only 0.1 ppm (12 Hz at 11.0T), which is smaller than the line-width achieved in the *in vivo* spectra. High-resolution spectra acquired from tissue acid extracts that would be capable of detecting such small differences did not show significant amounts of oxidized glutathione disulfide. Liquid chromatography and mass spectrometric assays of tumor tissue samples found oxidized glutathione disulfide <0.5% of the reduced form of glutathione. There may be regions of the tumor in which the oxidized form is present at higher levels, but overall the majority of the observed signal at 44.2 ppm is due to the reduced form of glutathione in these tumors.

The ability to detect serine labeled *in vivo* and multiple labeling *in vitro* allows us to probe another pathway in tumor biochemistry. The appearance of multiplets for the labeled serine (Fig. 4B) indicates that the tissue extract contains both single labeled and double-labeled species. Integration of the intensity of the central peak to the intensity of the two peaks on either side would reflect the relative abundance of singly or doubly labeled serine. The metabolism of [2-^{13}C]-glycine to [2-^{13}C]-serine occurs through the serine hydroxymethyltransferase pathway with the methylene group transferred from N^5,N^{10}-methylenetetrahydrofolate (m-THF) (21). When m-THF is generated with the methylene group donated from labeled [2-^{13}C]-glycine *via* the glycine cleavage system, label can appear in [3-^{13}C]-serine alone or in two serine carbons to yield [2,3-$^{13}C_2$]-serine. In normal tissue, the glycine cleavage system is confined within the mitochondria whereas the serine hydroxymethyltransferase pathway is available in both the cytosol and mitochondria. Integration of the central peak of the triplets shown in Fig. 4A to the flanking two peaks provides a measure of the relative contribution of the two pathways (21). Access to the m-THF pathway via labeling of the glycine pool may be helpful in assessing alterations in the activity of m-THF reductase, an enzyme central to folate metabolism. Increasing evidence shows that alterations in folate metabolism may be involved in carcinogenesis in a number of tissues (22). Interestingly, no labeling of serine was observed in human mammary MCF-7 cells treated with [2-^{13}C]-glycine indicating that this cell line lacks a functional glycine cleavage system (23). Whether this presence of the glycine cleavage system and serine hydoxymethyltransferase activity is unique to R3230Ac xenografts will be explored in future studies with these cells in culture.

The further metabolism of serine to cysteine is of particular importance as cysteine is typically identified as the limiting amino acid in glutathione synthesis (24). The ability of a tissue to supply its own cysteine through transsulfuration is key to understanding how glutathione levels may be altered to influence drug response. Although the enzymes required

for transsulfuration have been demonstrated to be expressed in a range of tumor cell lines (25), it is not clear in our studies whether ^{13}C-labeled tumor cysteine and glutathione originate from the presence of transsulfuration pathways in the tumor, or whether it originates in the liver and ^{13}C-labeled cyst(e)ine or (^{13}C-cys)-glutathione are then taken up by the tumor tissue. Circulating levels of glutathione are low and glutathione itself does not readily cross the cell membrane (24). However, many cancer cells possess γ-glutamyltranspeptidase activity which may offer a mechanism by which circulating glutathione components can be re-incorporated into the cellular biochemistry (24). The extract of liver tissue obtained from these rats show, as expected, active transsulfuration pathways resulting in label incorporation into the 2- and 3-positions of cysteinyl-glutathione and the both carbons of taurine. (Figure 4C). In the liver extract (Figure 4C, grey lines), the relative intensities of the two serine peaks and the visible ^{13}C-^{13}C scalar coupling in the [2-^{13}C]-serine peak at 57.4 and [3-^{13}C]-serine 61.3 ppm is reflected in the similar relative intensities and the presence of this coupling in the (^{13}C-cys)-glutathione-bimane peaks at 34.3 (3-^{13}C-cys)-GSH-bim and (2-^{13}C-cys)-GSH-bim at 53.8 ppm. This suggests that transsulfuration samples the entire serine pool to produce similarly labeled cysteine. The ^{13}C-^{13}C coupling is also seen in the taurine resonances at 48.5 and 36.4 ppm. In this case [2-^{13}C]-serine ends up as [2-^{13}C]-taurine and [3-^{13}C]-serine is metabolized to [1-^{13}C]-taurine. Unfortunately, the intensities of the (^{13}C-cys)-glutathione and taurine peaks are too low in the tumor extract spectra (e.g. Figure 4A) to definitively detect whether the ^{13}C-^{13}C scalar coupling in the serine resonances are preserved in these metabolites. The presence of components of the transsulfuration pathway has been observed in some cancer cells in culture (26,27), and in the NCI60 panel of human cancer cell lines (25) thus it is reasonable to hypothesize that a portion of the ^{13}C-labeled cysteine observed is generated in the tumor by transsulfuration. The transsulfuration pathway in R3230Ac tumor xenografts has not been previously reported and will be probed in future studies.

The studies presented here demonstrate the pathways that can be probed by observing the metabolism of [2-^{13}C]-glycine in both tumor and liver tissue. The R3230Ac tumors proved more challenging to study compared to the FSA tumors used previously due to the lower tissue glutathione content. Nonetheless, we have demonstrated how *in vivo* and *ex vivo* magnetic resonance experiments provide complementary information on the synthesis and distribution of glutathione in tumor tissue. Application of these methods to the study of therapy response has significant potential, due to the central role of glutathione in therapy response. For example, clinical studies have shown total glutathione levels tend to increase in non-responders and to remain constant or decrease in patients that respond to therapy (28). Our methods could eventually be used to non-invasively monitor such responses. Additionally the measurement of flux through metabolic pathways critical to glutathione production, such as formation of cysteine *via* transsulfuration, may offer new probes for drug targeting or monitoring therapy response.

Acknowledgments

Thanks to Dr. Mark Dewhirst of Duke University for providing the R3230Ac tumor line and for helpful discussions and to Dr. Nigel Deighton and Norm Glassbrook of the Genome Sciences Laboratory of NC State University for help with the acquisition and analyses of the mass spectrometry data. We would also like to thank Dr. Jeremy Flint of the University of Florida for his assistance with the setup and execution of the *in vivo* magnetic resonance studies.

This work was supported by grant R01CA114365 from the National Institutes of Health (M.P.G.) and by grant G0801239 from the Medical Research Council (P.E.T.).

Abbreviations used

CSI	chemical shift imaging
FSA	rat fibrosarcoma
GSH	reduced glutathione
GSSG	oxidized glutathione disulfide
HSQC	heteronuclear single quantum coherence spectroscopy
m-THF	N^5,N^{10}-methylenetetrahydrofolate
m/z	mass-to-charge ratio of detected analytes
R3230Ac	rat mammary adenocarcinoma

References

1. Kirlin WG, Cai J, Thompson SA, Diaz D, Kavanagh TJ, Jones DP. Glutathione redox potential in response to differentiation and enzyme inducers. Free Radical Biol Med. 1999; 27:1208–1218. [PubMed: 10641713]
2. Blair SL, Heerdt P, Sachar S, Abolhoda A, Hochwald S, Cheng H, Burt M. Glutathione metabolism in patients with non-small cell lung cancers. Cancer Res. 1997; 57:152–155. [PubMed: 8988057]
3. Barranco SC, Perry RR, Durm ME, Quraishi M, Werner AL, Gregorcyk SG, Kolm P. Relationship between colorectal cancer glutathione levels and patient survival: Early results. Dis Colon Rectum. 2000; 43:1133–1140. [PubMed: 10950013]
4. Joncourt F, Buser K, Altermatt H, Bacchi M, Oberli A, Cerny T. Multiple drug resistance parameter expression in ovarian cancer. Gynecol Oncol. 1998; 70:176–182. [PubMed: 9740686]
5. Barranco SC, Perry RR, Durm ME, Werner AL, Gregorcyk SG, Bolton WE, Kolm P, Townsend CM Jr. Intratumor variability in prognostic indicators may be the cause of conflicting estimates of patient survival and response to therapy. Cancer Res. 1994; 54:5351–5356. [PubMed: 7923164]
6. Gamcsik MP, Bierbryer R, Millis KK. Noninvasive monitoring of glutathione turnover in perfused MCF-7 cells. Free Radic Biol Med. 2004; 37:961–968. [PubMed: 15336312]
7. Gamcsik MP, Dubay GR, Cox BR. Increased rate of glutathione synthesis from cystine in drug-resistant MCF-7 cells. Biochem Pharmacol. 2002; 63:843–851. [PubMed: 11911835]
8. Gamcsik MP, Millis KK, Colvin OM. Noninvasive detection of elevated glutathione levels in MCF-7 cells resistant to 4-hydroperoxycyclophosphamide. Cancer Res. 1995; 55:2012–2016. [PubMed: 7743493]
9. Macdonald JM, Schmidlin O, James TL. In vivo monitoring of hepatic glutathione in anesthetized rats by ^{13}C NMR. Magn Reson Med. 2002; 48(3):430–439. [PubMed: 12210907]
10. Thelwall PE, Yemin AY, Gillian TL, Simpson NE, Kasibhatla MS, Rabbani ZN, Macdonald JM, Blackband SJ, Gamcsik MP. Noninvasive in vivo detection of glutathione metabolism in tumors. Cancer Res. 2005; 65:10149–10153. [PubMed: 16287997]
11. Bodenhausen G, Ruben DJ. Natural abundance nitrogen-15 NMR by enhanced heteronuclear spectroscopy. Chem Phys Lett. 1980; 69:185–189.
12. Manura JJ, Manura DJ. Isotope Distribution Calculator and Mass Spec Plotter. Scientific Instrument Services. 2009 www.sisweb.com/mstools/isotope.htm.
13. Vukovic V, Nicklee T, Hedley DW. Microregional heterogeneity of non-protein thiols in cervical carcinomas assessed by combined use of HPLC and fluorescence image analysis. Clin Cancer Res. 2000; 6(5):1826–1832. [PubMed: 10815904]
14. Dringen R, Verleysdonk S, Hamprecht B, Willker W, Leibfritz D, Brand A. Metabolism of glycine in primary astroglial cells: Synthesis of creatine, serine and glutathione. J Neurochemistry. 1998; 70:835–840.
15. Finkelstein JD. Methionine metabolism in mammals. J Nutr Biochem. 1990; 1:228–237. [PubMed: 15539209]

16. Gamcsik MP. ^{13}C-Isotopic Enrichment of Glutathione in Cell Extracts Determined by Nuclear Magnetic Resonance Spectroscopy. Anal Biochem. 1999; 266:58–65. [PubMed: 9887213]

17. Schroeder T, Yuan H, Viglianti BL, Peltz C, Asopa S, Vujaskovic Z, Dewhirst MW. Spatial heterogeneity and oxygen dependence of glucose consumption in R3230Ac and fibrosarcomas of the Fischer 344 Rat. Cancer Res. 2005; 65:5163–5171. [PubMed: 15958560]

18. Vukovic V, Nicklee T, Hedley DW. Multiparameter fluorescence mapping of nonprotein sulfhydryl status in relation to blood vessels and hypoxia in cervical carcinoma xenografts. Int J Radiat Oncol Biol Phys. 2002; 52:837–843. [PubMed: 11849809]

19. Hedley DW, Nicklee T, Moreno-Merlo F, Pintilie M, Fyles A, Milosevic M, Hill RP. Relations between non-protein sulfydryl levels in the nucleus and cytoplasm, tumor oxygenation, and clinical outcome of patients with uterine cervical carcinoma; glutathione; cysteine; mercury orange; thiol; Int J Radiat Oncol Biol Phys. 2005; 61:137–144. [PubMed: 15629604]

20. Allen RG, Balin AK. Effects of oxygen on the antioxidant responses of normal and transformed cells. Exp Cell Res. 2003; 289:307–316. [PubMed: 14499631]

21. Cowin GJ, Willgoss DA, Bartley J, Endre ZH. Serine isotopomer analysis by ^{13}C-NMR defines glycine-serine interconversion in situ in the renal proximal tubule. Biochim Biophys Acta. 1996; 1310:32–40. [PubMed: 9244172]

22. Larsson SC, Giovannucci E, Wolk A. Folate intake, MTHFR polymorphisms, and risk of esopogeal, gastric, and pancreatic cancer: a meta analysis. Gastroenterology. 2006; 131:1271–1283. [PubMed: 17030196]

23. Fu TF, Rifer JP, Schirch V. The role of serine hydroxymethyltransferase isozymes in one-carbon metabolism in MCF-7 cells as determined by ^{13}C NMR. Arch Biochem Biophys. 2001; 393:42–50. [PubMed: 11516159]

24. Meister, A. A brief history of glutathione and a survey of its metabolism and functions. In: Dolphin, D.; Poulson, R.; Avramovic, O., editors. Glutathione Chemical Biochemical and Medical Aspects, Part A. Volume III, Coenzymes and Cofactors. New York: John Wiley & Sons; 1989. p. 1-48.

25. Zhang W, Braun A, Bauman Z, Olteanu H, Madzelan P, Banerjee R. Expression profiling of homocysteine junction enzymes in the NCI60 panel of human cancer cell lines. Cancer Res. 2005; 65:1554–1560. [PubMed: 15735045]

26. Kandil S, Brennan L, McBean GJ. Glutathione depletion causes a JNK and p38(MAPK)-mediated increase in expression of cystathionine-gamma-lyase and upregulation of the transsulfuration pathway in C6 glioma cells. Neurochem Int. 2010; 56:611–619. [PubMed: 20060865]

27. Prudova A, Albin M, Bauman Z, Lin A, Vitvitsky V, Banerjee R. Testosterone regulation of homocysteine metabolism modulates redox status in human prostate cancer cells. Antioxid Redox Signal. 2007; 9:1875–1881. [PubMed: 17854288]

28. Cheng X, Kigawa J, Minigawa Y, Kanamori Y, Itamochi H, Okada M, Terakawa N. Glutathione S-transferase-π expression and glutathione concentration in ovarian carcinoma before and after chemotherapy. Cancer. 1997; 79:521–527. [PubMed: 9028363]

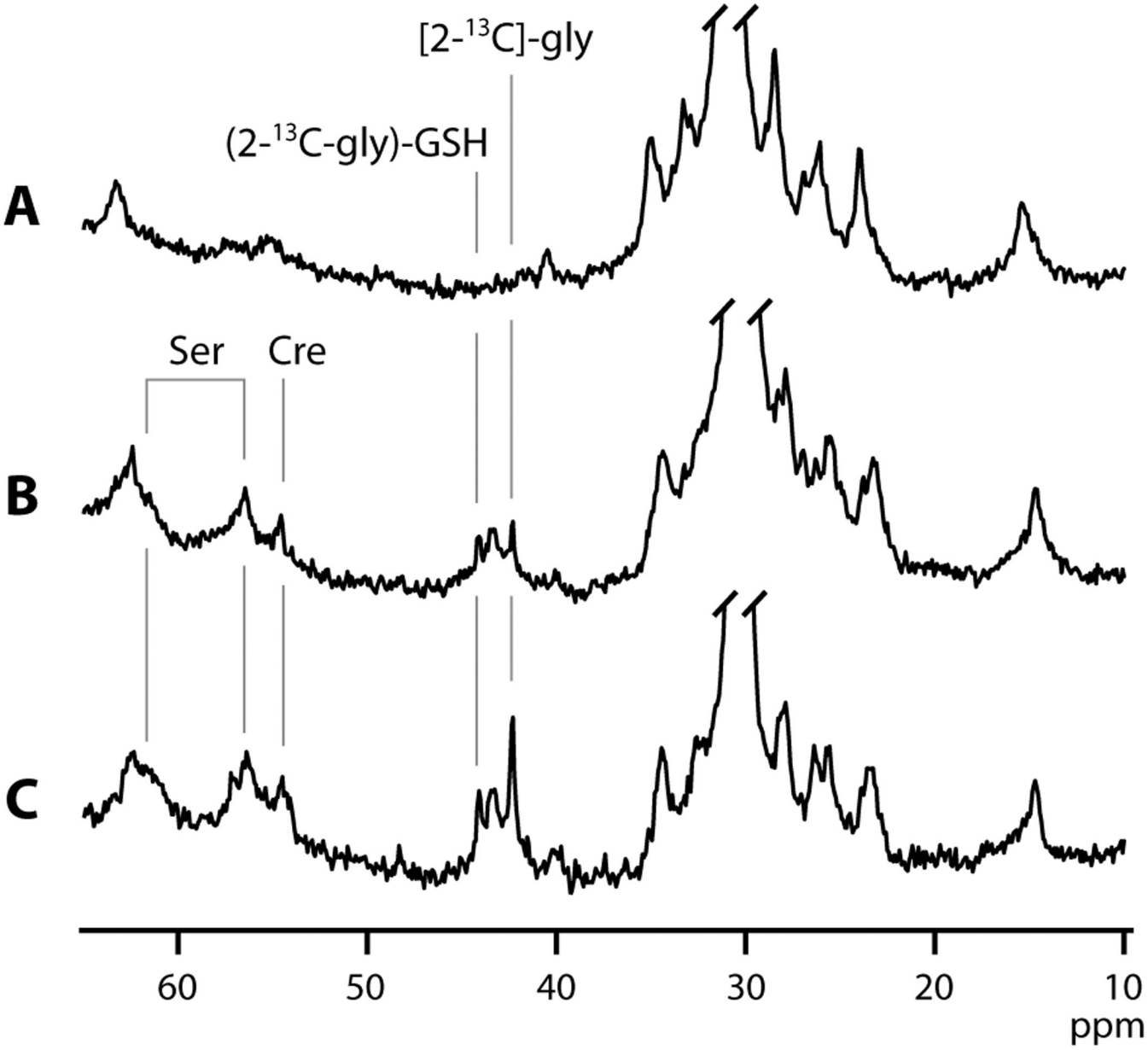

Figure 1.

In vivo non-localized ^{13}C spectra from a subcutaneously implanted R3230Ac tumor before (A) and after 30 hours (B) of [2-^{13}C]-glycine infusion at a rate of 0.5 mmol/kg/h. (C) A spectrum from an analogous study employing [2-^{13}C]-glycine infusion at a higher rate of 1 mmol/kg/h. [2-^{13}C]-glycine ([2-^{13}C]-gly) appears at 42.4 ppm, and incorporation into the glycinyl-residue of glutathione ((2-^{13}C-gly)-GSH) is visible at 44.2 ppm. Also detected are labels in two carbons of serine, [2-^{13}C]-ser and [3-^{13}C]-ser and creatine, ([2-^{13}C]-creatine).

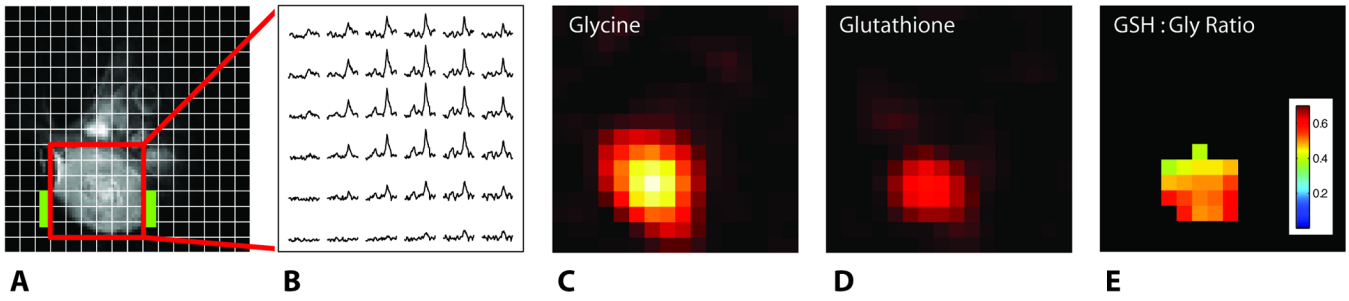

Figure 2.

In vivo ^{1}H image of a R3230Ac tumor (A) and ^{13}C 2D-CSI data showing glutathione and glycine resonances (B). The location of the ^{13}C coil is indicated in green on the ^{1}H image. Maps of detected labeled glycine, [2-^{13}C]-gly (C) and glutathione, (2-^{13}C-gly)-GSH (D), and the ratio of ^{13}C-labeled glutathione:glycine (GSH:Gly), were generated from integrated peak areas from this 2D-CSI dataset.

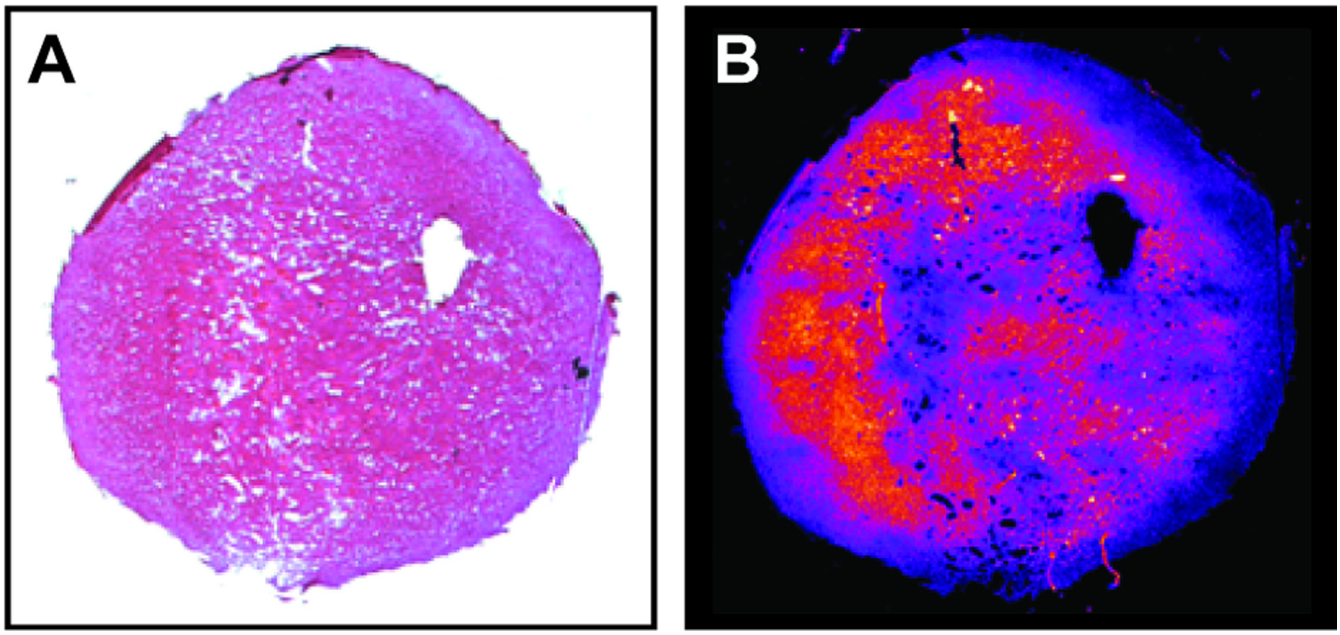

Figure 3.
Histological sections from an R3230Ac stained with Hematoxylin-Eosin (A) and the fluorescent glutathione reagent Mercury Orange (B).

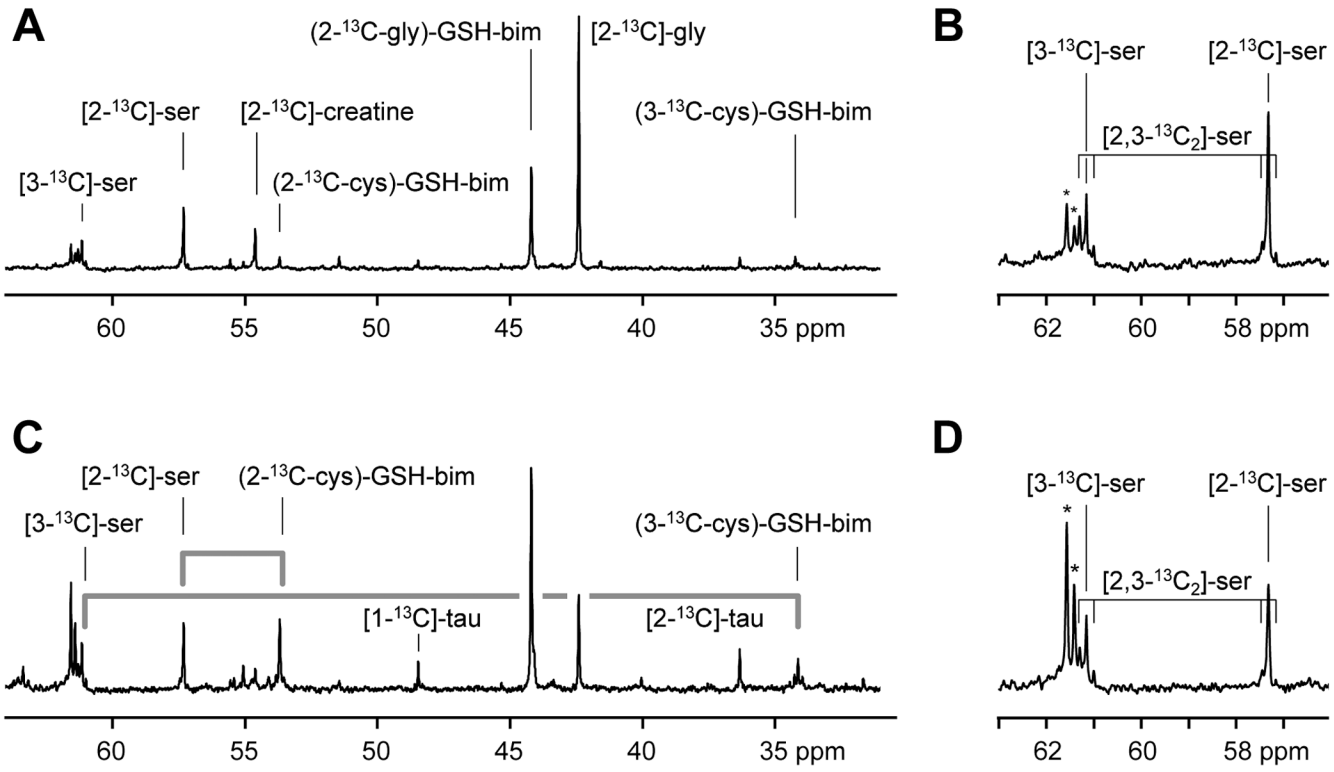

Figure 4.

High resolution ^{13}C magnetic resonance spectra acquired from monobromobimane treated acid extracts of tumor (A, B) and liver (C, D) tissue samples taken from rats infused with [2-^{13}C]-glycine at 1 mmol/kg/h for 24 h. The appearance of the label in the 2-carbon of the glycinyl-residue of glutathione-bimane (2-^{13}C-gly)-GSH-bim, the 2-carbon of the cysteinyl-residue ((2-^{13}C-cys)-GSH-bim) and the 3-carbon of the cysteinyl-residue ((3-^{13}C-cys)-GSH-bim) are detected. The fate of the serine ^{13}C-labels as they are metabolized through the transsulfuration pathway and appear in the cysteinyl-carbons of glutathione are indicated by the grey lines. Additional resonances are visible from taurine (tau). An expansion of the region around the serine peaks is shown (B,D). These show the presence of singly labeled [3-^{13}C]-serine and [2-^{13}C]-serine and smaller amounts of [2,3-$^{13}C_2$]-serine. The asterisks indicate peaks due to natural abundance glucose in the extracts.

Table I

Metabolite Levels in R3230Ac Tumors

Infusate (mmol/kg/h)	Infusion Time (h)	GSH	Cysteine	Glycine	Serine
		(μmol/g-tissue)			
Control (n = 4)		1.22 ± 0.28	0.175 ± 0.070	2.80 ± 0.57	0.872 ± 0.138
0.5 (n = 6)	31–46	1.31 ± 0.43	0.142 ± 0.035	4.52 ± 1.00	1.43 ± 0.55
1.0 (n = 3)	24	1.29 ± 0.24	0.195 ± 0.016	5.96 ± 0.96	1.52 ± 0.38